PAPER • OPEN ACCESS

New adhesive strength evaluation method based on the singular stress field considering three-dimensional geometry

To cite this article: N-A Noda 2019 *IOP Conf. Ser.: Mater. Sci. Eng.* **629** 012029

New adhesive strength evaluation method based on the singular stress field considering three-dimensional geometry

N-A Noda[1,2]

[1]Mechanical Engineering Department, Kyushu Institute of Technology, 1-1 Sensui-cho Tobata-ku, Kitakyushu-shi, 804-8550, Japan

E-mail: noda.naoaki844@mail.kyutech.jp

Abstract. Adhesive joints are widely used although different materials properties cause the singular stress field whose intensity is controlled by the adhesive joint geometry. Our previous studies showed that debonding strength can be expressed as a constant value of the critical intensity of singular stress field (ISSF) by applying two-dimensional modelling. By considering the real adhesive geometry, in this study, the ISSFs along the interface edge of three-dimensional prismatic butt joints are considered by varying the adhesive thicknesses. It is found that the critical ISSF in 3D modelling is almost constant independent of the adhesive thickness. The magnitude and position of the maximum ISSF are discussed by varying the corner fillet radius in comparison with two-dimensional modelling.

1. Introduction

Adhesive joints have several advantages such as light weight and low cost compared with the other traditional joints. Therefore, adhesive joints are widely used in various industrial fields [1-3]. However, different material properties cause singular stresses at the interface end, which may lead to debonding failure in structures [4-12].

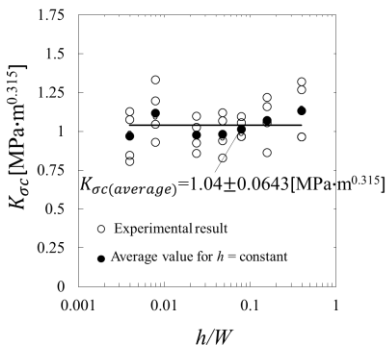

Figure 1. Adhesive strength for S35C / Epoxy resin expressed as a constant critical ISSF $K_{\sigma c}$ by using 2D model.

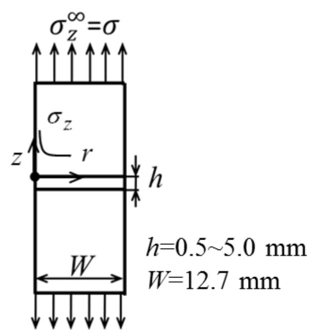

Figure 2. 2D butt joint modelling.

The bonded strength is closely related to the intensity of the singular stress field (ISSF). Recent previous studies showed that the debonding strength can be expressed as a constant value of ISSF as shown in figure 1 [12, 13]. In those studies, the ISSF was analyzed by using two-dimensional modelling assuming plane strain as shown in figure 2. Suzuki [14] studied the adhesive bonded strength when medium carbon steel plates are bonded by epoxy resin. His experimental results are used widely in research since the experiment was conducted carefully with high accuracy. In this study, therefore, Suzuki's specimen in figure 3 [14] will be analysed by considering the three-dimensional prismatic butt joint geometry. Then, the ISSF distribution will be discussed along the adhesive interface edge by extending the mesh independent technique proposed previously [7-13].

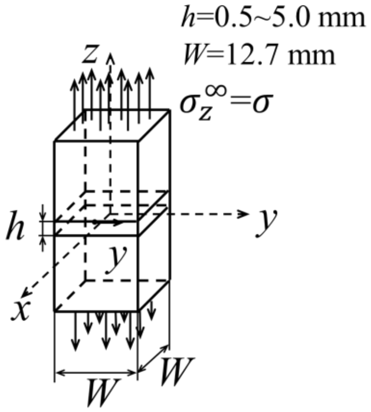

Figure 3. 3D prismatic butt joint.

2. FEM stress distribution along the adhesive interface

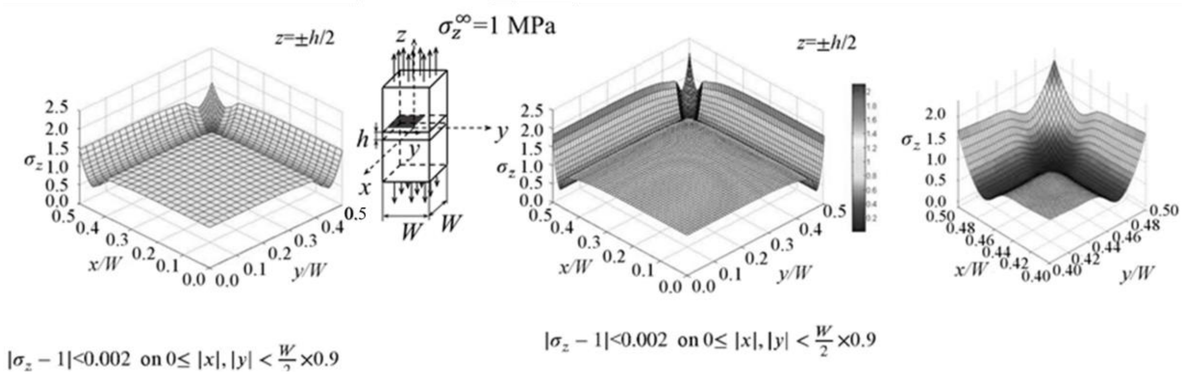

(a) Large mesh (b) Small mesh (c) Detail of x/W, y/W = 0.4~0.5

Figure 4. FEM stress distribution σ_z of 3D prismatic butt joint on $z = \pm h/2$.

In this study, the finite element method (FEM) is applied to adhesive strength analysis. The FEM has been used in wide engineering fields such as composite materials [7-13], impact strength [15], and complicated structures including traditional joints [16]. figure 4 shows an example of FEM stress distributions along the adhesive interface in prismatic butt joint when h/W=0.1. This result is corresponding to one of Suzuki's specimens [14]. The mild steel S35C has Young's modulus E=210GPa and Poisson's ratio ν=0.3 and the epoxy resin has E=3.14GPa and ν=0.37. As shown in figure 4, in the interior region of the interface 0≤x, y<0.45, FEM stress is accurate since they are independent of the minimum mesh size e_{min} and satisfy $|\sigma_z\text{-}1|$<0.002 under the remote tensile stress σ_z^∞=1. However, FEM stress values are not accurate near the interface side $|x|$=0.5 and $|y|$=0.5 since they varies depending on the mesh size e_{min}. It should be noted that the real interface stress should go to infinity along the interface side $|x|$=0.5 and $|y|$=0.5. In this study, the intensity of this singular stress field (ISSF) is obtained by applying mesh independent technique. Since the ISSF varies depending on the location and also the adhesive thickness, the ISSF distributions will be discussed in the next section. In this study, the mesh independent technique coupled with FEM is extended to the three dimensional prismatic butt joints. The details may be found in [7-13, 17]. This new method can be applied to real adhesive joints to evaluate the adhesive strength.

3. ISSF distribution and critical ISSF distribution when debonding occurs

figure 5 shows the ISSF distributions along the interface side K_σ^{Side} under remote tensile stress $\sigma_z^\infty = 1$. The ISSF K_σ^{Side} is defined by eq.(1).

$$K_\sigma^{Side} = \lim_{r\to 0}\left[r^{1-\lambda} \times \sigma_z^{Side,Real}(r,y)\right] \tag{1}$$

The ISSF K_σ^{Side} decreases with decreasing the adhesive thickness. Each ISSF distribution is almost constant at the most portion except near the vertex. The detail of ISSF around the vertex is shown in figure 5(b), (c). In figure 5 (c), as shown by the dotted lines in the range of 0.4995≤y≤0.5, the ISSFs go to infinity because different singular stress field exists at the vertex [18, 19].

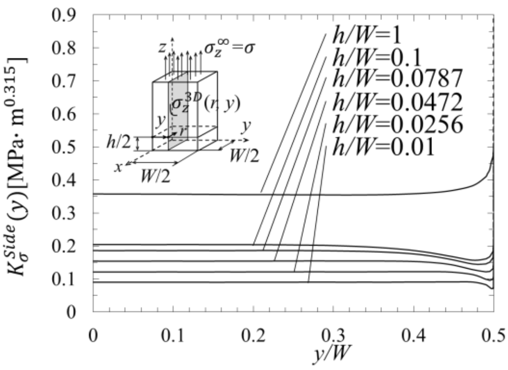

(a) ISSF distributions of 3D butt joint

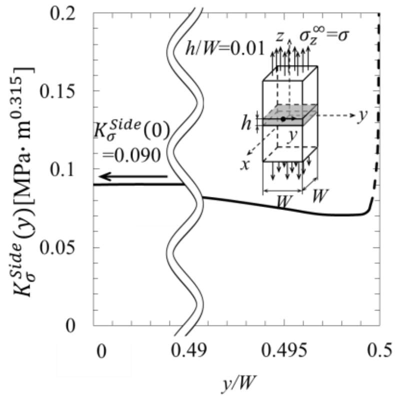

(b) Detail of around the vertex when h/W = 0.01

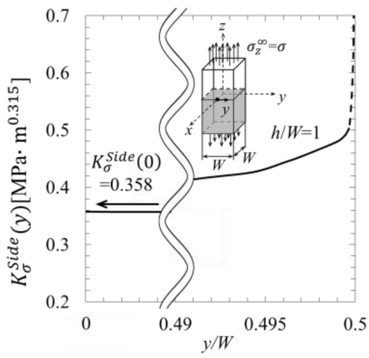

(c) Detail of around the vertex when h/W = 1

Figure 5. ISSF distribution $K_\sigma^{Side}(y)$ of 3D butt joint under σ_z^∞ = 1 MPa.

figure 6(a) shows the critical ISSF distributions of $K_{\sigma c}^{Side}(y)$ under remote tensile stress $\sigma_z^\infty = \sigma_c$ when the debonding occurs. figure 6(b) shows the detail of $K_{\sigma c}^{Side}(y)$ at 0.49≤y≤0.5. As shown in figure 6(a), the critical ISSF distributions are quite similar and they are in a narrow band region. It should be noted that the critical value of the ISSF in the middle side region in figure 6 (a) is almost the same of the value obtained by 2D modelling in figure 1.

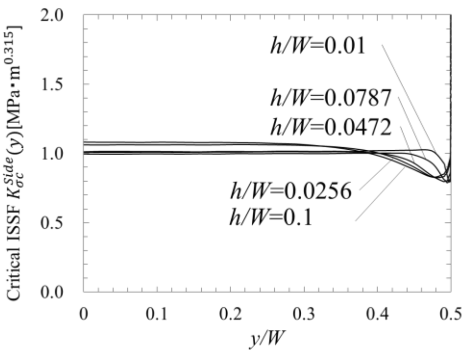

(a) Critical ISSF distribution

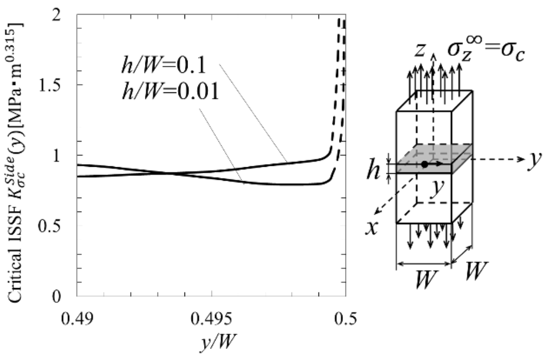

(b) Detail of around the vertex when h/W=0.1 and 0.01

Figure 6. Critical ISSF distributions $K_{\sigma c}^{Side}(y)$ when debonding occurs under $\sigma_z^\infty=\sigma_c$.

4. ISSF distribution of fillet corner

In reality, there is no sharp corner and usually there is a small fillet radius at the corner as shown in figure 7. The local polar coordinate along the interface as shown in figure 7 is used to describe the position along the fillet by changing the fillet radius ρ under the same adhesive thickness h/W= 0.01.

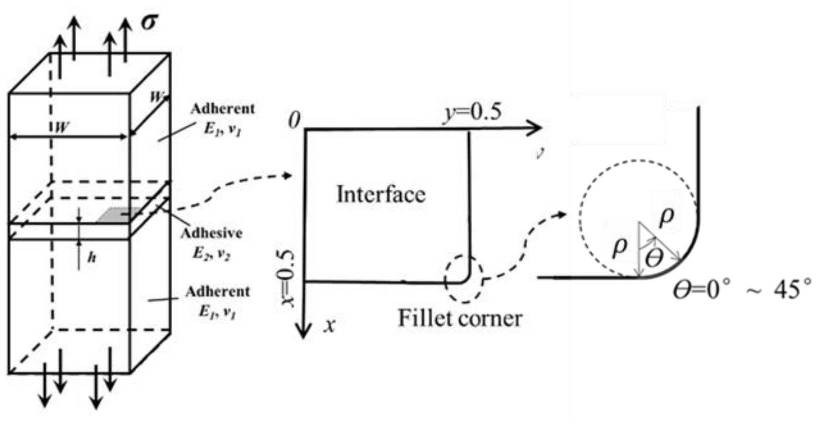

Figure 7. Prismatic butt joint model with fillet considered in this study.

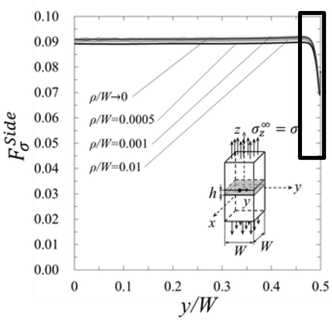

(a) When ρ/W=0~0.01

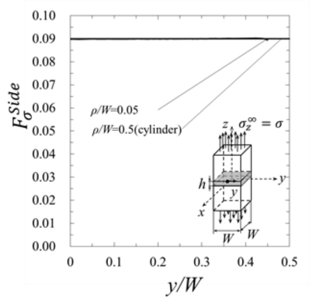

(b) When ρ/W=0.05~0.5

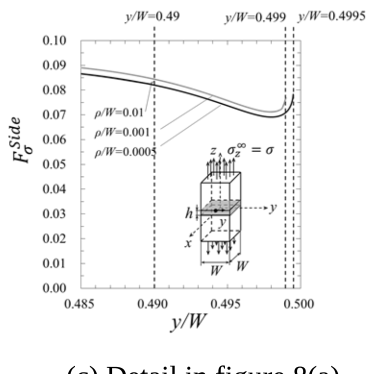

(c) Detail in figure 8(a)

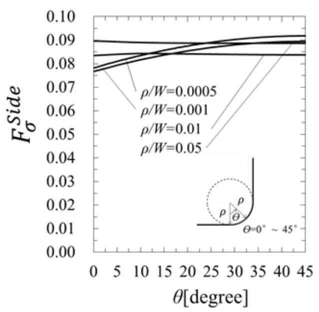

(d) Detail at fillet in figure 8(a)

Figure 8. ISSF distributions in figure 7 along the edge of fillet.

figure 8 show the ISSF distribution along the interface corner when the relative roundness of the fillet ρ/W is changed as ρ/W = 0, 0.0005, 0.001, 0.01, 0.05. It is found that the maximum value of the intensity ISSF occurs around y/W≈0.46 in most cases. The corner of the specimen is always chamfered, and ρ can be regarded as the minimum chamfer size in practical use, therefore $\rho \geq 0.2$ mm should be considered. Therefore, for Suzuki's specimen width W = 12.7 mm in figure 3, $\rho/W \geq 0.016$. figure 9 shows an example of the fractured surface in [14]. The fractured origin looks close to the position of the maximum ISSF. figure 8 shows the minimum ISSF occurs around y/W ≈0.498 in most cases. The variation of the ISSF is less than 1% when $\rho/W\geq0.05$ and less than 10% even when $\rho/W\geq0.0005$. It may be concluded that the effect of the fillet radius ρ of the ISSF is relatively small.

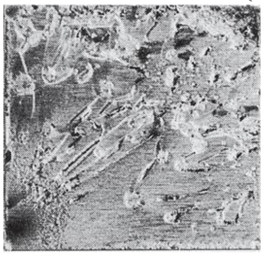

Figure 9. Fracture surface when h/W=0.00787 (h = 0.1 mm, W = 12.7 mm) in figure 3.

5. Conclusion

In this study, the ISSF distributions along the interface edge of three-dimensional joints were discussed by considering the real specimen geometry for various adhesive thicknesses. The magnitude and position of the maximum ISSF were investigated by varying the corner fillet radius in comparison with two-dimensional modelling. The following conclusions can be drawn from that discuss.

(1) The ISSF distribution along the interface edge is almost constant except near the vertex. The ISSF value decreases with decreasing the adhesive thickness.
(2) The critical ISSF distributions when the debonding occurs are almost the same independent of the adhesive thickness.
(3) It is found that the maximum value of the intensity ISSF occurs around y/W≈0.46 in most cases.

References

[1] Barnes T A and Pashby I R 2000 Joining techniques for aluminum spaceframes used in automobiles: part II - adhesive bonding and mechanical fasteners *J Mater Process Technol* **99** 72-9
[2] Higgins A 2000 Adhesive bonding of aircraft structures *Int J Adhes* **20** 367-76
[3] Petrie E M 2008 Adhesives for the assembly of aircraft structures and components: decades of performance improvement, with the new applications of the horizon *Metal Finish* **106** 26-31
[4] Qian Z and Akisanya A R 1998 An experimental investigation of failure initiation in bonded joints *Acta Mater* **46** 4895-904
[5] Akisanya A R and Meng C S 2003 Initiation of fracture at the interface corner of bi-material joints *J Mech Phys Solids* **51** 27-46
[6] Mintzas A and Nowell D 2012 Validation of an Hcr-based fracture initiation criterion for adhesively bonded joints *Eng Fract Mech* **80** 13-27
[7] Zhang Y, Noda N A, Takaishi K T and Lan X 2011 Effect of adhesive thickness on the interface of singular stress at the adhesive dissimilar joint *Transactions of the Japan Society of Mechanical Engineers Series A* **77** 360-72
[8] Zhang Y, Noda N A, Wu P Z and Duan M L 2015 A mesh-independent technique to evaluate stress singularities in adhesive joints *Int J Adhes Adhes* **57** 105-17
[9] Zhang Y, Noda N A, Wu P and Duan M 2015 Corrigendum to "A mesh-independent technique to evaluate stress singularities in adhesive joints" *Int J Adhes Adhes* **60** 130
[10] Miyazaki T, Noda N A, Li R, Uchikoba T and Sano, Y 2013 Debonding criterion for single lap joints from the intensity of singular stress field *Transactions of The Japan Institute of Electronics Packaging* **16** 143-51 (in Japanese)

[11] Miyazaki T, Noda N A, Uchikoba T, Li R and Sano Y, 2014 Proposal of a convenient and accurate method for evaluation of debonding strength *Trans Soc Autom Eng Jpn* **45** 895-901 (in Japanese)
[12] Noda N A, Miyazaki T, Li R, Uchikoba T, Sano Y and Takase Y 2015 Debonding strength evaluation in terms of the intensity of singular stress at the corner with and without fictitious crack *Int J Adhes Adhes* **61** 46-64
[13] Noda N A, Miyazaki T, Uchikoba T, Li R, Sano Y and Takase Y 2014 Convenient debonding strength evaluation based on the intensity of singular stress for adhesive joints *Transactions of The Japan Institute of Electronics Packaging* **17** 132-42 (in Japanese)
[14] Suzuki Y 1987 Adhesive tensile strengths of scarf and butt joints of steel plates (relation between adhesive layer thicknesses and adhesive strengths of joints) *JSME. Int. J.* **30** 1042-51
[15] Noda N A, Shen Y, Takaki R, Akagi D, Ikeda T, Sano Y and Takase Y 2017 Relationship between strain rate concentration factor and stress concentration factor *Theor Appl Fract Mec* **90** 218-27
[16] Noda N A, Chen X, Sano Y, Wahab M A, Maruyama H, Fujisawa R and Takase Y 2016 Effect of pitch difference between the bolt-nut connections upon the anti-loosening performance and fatigue life *Mater Design* **96** 476-89
[17] Marc Mentat team 2012 Theory and User Information A *MSC Software* Tokyo 713
[18] Koguchi H and Nakazima M 2010 Influence of adhesive layer thickness on intensity of stress singularity at a vertex in three-dimensional joints with three layers: In case of external loading *Transactions of the Japan Society of Mechanical Engineers Series A* **76** 1110-8 (in Japanese)
[19] Miyazaki T, Inoue T, Noda N A and Sano Y 2018 A precise and efficient method for evaluating singular stress field at the vertex in three dimensional bonded body *Transactions of the JSME* **84** 1-17 (in Japanese)